Mechanism of Binding of Multivalent Immune Complexes to Fc Receptors. 2. Kinetics of Binding†

Steven K. Dower,* Julie A. Titus,‡ Charles DeLisi, and David M. Segal

ABSTRACT: The kinetics of association and dissociation of affinity cross-linked IgG oligomers with Fc receptors on P388D_1 cells have been studied at 0 °C. For dimers prepared with two different affinity cross-linking reagents (DIBADL and BDPE) and also trimers and a heavy oligomer fraction prepared with BDPE, monomeric IgG accelerates the rate of dissociation of bound oligomer from the cells. This observation is consistent with a binding mechanism in which monovalently, and multivalently bound species are in rapid equilibrium with one another on the cell surface and in which the rate of formation of the divalently bound species is faster than the dissociation of the monovalent species from the cells. As predicted, the rates of dissociation of BDPE cross-linked oligomers decrease with size, and dimers (cross-linked with DIBADL) which can self-aggregate on the cell surface dissociate more slowly than nonaggregating (BDPE) dimers. The association and dissociation of oligomers with P388D_1 cells proceed by parallel fast and slow processes, even with cells that bind dimers with a single affinity. The origin of this heterogeneity is not known but could arise from a fraction of receptors in environments with limited accessibility to bulk solution. The fast component of the association reaction is second order, and the rate-limiting step of this process is the formation of the monovalently bound intermediate from solution-phase oligomer.

In our previous paper [Dower et al. (1981) preceding paper in this issue], we presented an analysis of the mechanism of equilibrium binding of multivalent IgG model immune complexes to the Fc receptors on cells from the mouse macrophage line P388D_1. While this yielded considerable insight into the mechanism of multivalent binding, it is unlikely that the binding of immune complexes by cells bearing Fc receptors reaches equilibrium in vivo. More probably, binding is a steady-state process which precedes other cellular events, such as internalization and degradation (Silverstein et al., 1977). In order to further our understanding of the adaptor role of antibodies in the processing of antigens by effector cells, we have, in this paper, characterized the kinetics of interaction of IgG oligomers with Fc receptors on metabolically inhibited P388D_1 cells. These studies provide support for the multivalent mechanism described in the preceding paper in this issue (Dower et al., 1981) and define the rate-limiting processes in oligomer binding.

Experimental Procedures

Binding and Kinetic Measurements. The binding assay and the protein and cell samples used in these studies are described in the preceding paper in this issue (Dower et al., 1981). The association of ^{125}I-labeled dimer with ^{51}Cr-labeled P388D_1 cells was initiated by adding cells to premixed protein solutions at 0 °C. The average number of 7S IgG subunits bound per cell was determined at various times by using the phthalate oil method (Segal and Hurwitz, 1977) but with the centrifugation time for the oil tubes reduced to 10 s.

The dissociation of ^{125}I-labeled oligomers from P388D_1 cells was measured by first equilibrating cells with the labeled oligomers at 0 °C. Cells were pelleted by centrifugation, and the supernatant solution was removed by aspiration. The dissociation was initiated by resuspending the cells at 0 °C, either in medium alone or in medium containing unlabeled protein. Cell-bound ^{125}I-labeled protein was then measured by the phthalate oil method with a 10-s centrifugation. The medium used in these experiments was balanced salt solution containing 2.5% BSA[1] and 0.2% sodium azide, pH 7.4. The average number of 7S subunits of oligomers bound per cell (r) was calculated as described previously (Jones et al., 1979), and data were analyzed by using MLAB (Knott, 1979).

Theory

In the preceding paper in this issue (Dower et al., 1981) we showed that the binding at equilibrium of IgG oligomers to Fc receptors on P388D_1 cells is described by a simple multivalent mechanism. This mechanism also predicts characteristic features for the kinetics of interaction of IgG oligomers with these cells (DeLisi, 1978). For an IgG dimer, binding occurs in two sequential steps:

$$D + R_f \underset{k_{-1}}{\overset{2k_1}{\rightleftharpoons}} D_1 \qquad (1A)$$

$$D_1 + R_f \underset{2k_{-2}}{\overset{k_2}{\rightleftharpoons}} D_2 \qquad (1B)$$

In the first step, solution-phase dimer, D, at concentration D (in molar units) reacts with free receptor, R_f, at concentration R_f (in cell surface concentration units) to form monomerically bound dimer, D_1, at concentration D_1 (in cell surface concentration units). The monomeric binding step has a second-order forward rate constant $2k_1$ and a first-order reverse rate constant k_{-1}. In the second step D_1 reacts with another free receptor to form the dimerically bound species D_2, with a second-order forward rate constant k_2 and a first-order reverse rate constant $2k_{-2}$. The factors of 2 in $2k_1$ and $2k_{-2}$ arise from statistical effects, which have been dis-

† From the Immunology Branch and Laboratory of Theoretical Biology, National Cancer Institute, National Institutes of Health, Bethesda, Maryland 20205. *Received March 26, 1981.*

‡ This paper represents partial fulfillment of the requirements for the degree of Doctor of Philosophy in the Department of Biochemistry, The George Washington University, Washington, DC.

[1] Abbreviations used: BDPE, bis(2,4-dinitrophenyl)pimelic ester; BDPE oligomers, oligomers of anti-Dnp antibodies cross-linked with BDPE; DIBADL, bis(α-bromoacetyl-ϵ-Dnp-Lys-Pro)ethylenediamine; DIBADL oligomers, oligomers of anti-Dnp antibodies cross-linked with DIBADL; Dnp, 2,4-dinitrophenyl; DNA, deoxyribonucleic acid; BSA, bovine serum albumin; $NaDodSO_4$, sodium dodecyl sulfate.

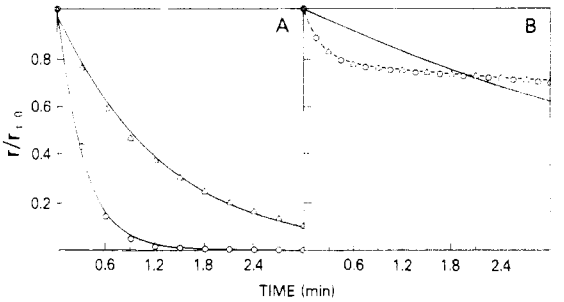

FIGURE 1: Simulated dissociation of dimeric IgG in the presence and absence of monomeric IgG. The points were calculated from the differential equation model (eq 3A–D) in the absence (△) and the presence (○) of 2×10^{-5} M monomer. The continuous curves are "best fit" by using one (—) or two (- - -) exponentials. Parameter values used in the simulation were $k_1 = 6 \times 10^6$ M^{-1} min^{-1} and $k_{-1} = 4.7$ min^{-1}; in (A) $k_{-2} = 4.7$ min^{-1} and $k_2R_0 = 62$ min^{-1} (rapid cross-linking); in (B) $k_{-2} = 0.019$ min^{-1} and $k_2R_0 = 0.25$ min^{-1} (slow cross-linking). $r_{t=0}/r_0$ was set at 0.506 in all cases, where $r_{t=0}$ is the amount of dimer bound at time zero and r_0 is receptors per cell.

cussed previously (Dower et al., 1981).

A characteristic feature of this mechanism is that D_1 can either dissociate from the cell surface with rate k_{-1} or form D_2 with rate k_2R_f. The net rate of dissociation of dimer from the cell surface will therefore depend on R_f. In the experiments described in this paper, we have depleted free receptor by adding monomeric IgG to the medium in which cells bearing radiolabeled dimers were suspended. The binding of monomer is described by

$$M + R_f \underset{k_{-1}}{\overset{k_1}{\rightleftharpoons}} M_1 \tag{2}$$

where M and M_1 are the concentrations of solution phase monomer M and bound monomer M_1, respectively. The kinetic behavior of the system can be described by the set of differential equations:

$$dD_1/dt = 2k_1DR_f + 2k_{-2}D_2 - k_{-1}D_1 - k_2D_1R_f \tag{3A}$$

$$dD_2/dt = k_2D_1R_f - 2k_{-2}D_2 \tag{3B}$$

$$dM_1/dt = k_1MR_f - k_{-1}M_1 \tag{3C}$$

$$dR_f/dt = 2k_{-2}D_2 + k_{-1}D_1 + k_{-1}M - 2k_1DR_f - k_2D_1R_f - k_1MR_f \tag{3D}$$

The steady-state approximation $dD_1/dt = 0$ with the additional constraints that $D = 0$ and $D_2 \gg D_1$ shows how the net rate of dimer release depends upon R_f

$$k_r = \frac{2k_{-1}k_{-2}}{k_2R_f + k_{-1}} \tag{4}$$

where k_r is the steady-state rate constant for dimer dissociation. Equation 4 shows that the rate of dissociation of dimeric ligand will increase as R_f decreases, provided that $k_2R_f > k_{-1}$. Thus, monomeric IgG will accelerate dimer release only when the rate at which $D_1 \rightarrow D_2$ is greater than the rate at which D_1 dissociates from the cell.

Simulations of the time dependence of dimer binding or dissociation using eq 3A–D produced curves which could be closely approximated with simple exponential functions. The results of one such simulation are shown in Figure 1. In Figure 1A the parameter values used were selected so that the cross-linking rate ($D_1 \rightarrow D_2$) was faster than the rate of dimer dissociation from the cell surface ($D_1 \rightarrow D$). It can be seen that under these conditions, the simulated points are closely fit by a single exponential, and the occupancy of receptors by monomeric IgG leads to an enhanced rate of dimer dissociation. If, however, the cross-linking rate is slow compared with the rate of monomer dissociation (Figure 1B), the simulated dissociation pattern cannot be fit by a single exponential. In this case, however, the rate of dissociation is unaffected by changing the free receptor concentration. Since in all cases the behavior predicted by the model could be fit by no more than two exponentials, we analyzed our data with equations of the form

$$B^r = B_A{}^r e^{-k_A{}^r t} + B_B{}^r e^{-k_B{}^r t} \tag{5}$$

for dissociation reactions, and

$$B^f = B_A{}^f(1 - e^{-k_A{}^f t}) + B_B{}^f(1 - e^{-k_B{}^f t}) \tag{6}$$

for association. The relationships between the empirical rate constants determined from fits to eq 5 and 6 with those of the model (eq 1 and 2) will be treated under Discussion.

Equation 6 approximates the association reactions because the experiments described in this paper were done under pseudo-first-order conditions (i.e., D remained nearly constant during the course of the experiment). The pseudo-first-order rate constants obtained from eq 6 are related to the empirical second-order forward rate constant, $\bar{k}^f$, and the first-order reverse rate constant $\bar{k}_r$, by eq 7. Values for $\bar{k}^f$ and $\bar{k}^r$ were

$$k^f = \bar{k}^f D + \bar{k}^r \tag{7}$$

determined from the slopes and intercepts of k^f vs. D plots (Jencks, 1969).

Results

Kinetics of Interaction of BDPE Cross-Linked Dimer with P388D$_1$ Cells at 0 °C. The association of radiolabeled BDPE dimer with $P388D_1$ cells at 0 °C was initiated by adding cells to medium containing four different concentrations of ^{125}I-labeled protein, and the amounts of cell-bound dimer were determined as a function of time by using the phthalate oil separation method. The results of such an experiment (Figure 2) show that, at the lowest dimer concentration used (2.1×10^{-9} M), the system reached equilibrium within 2 h. Since the free dimer concentrations did not decrease detectably (i.e., by more than 5%) as a result of binding to the cells, the experiments were performed under pseudo-first-order conditions. Quantitative analysis of the dimer association data in Figure 2 showed that these were poorly fit with one exponential but were well fit by two (eq 6) and that using three did not significantly improve the fit. Approximately 65% of the binding process occurred at the fast rate (Figure 2B). A plot of the observed rate constant against the free dimer concentration is shown in Figure 2C. The observed rate constant increases linearly with the dimer concentration showing that the fast phase of the reaction is second order. From the slope of the line in Figure 1C the forward rate constant for the fast phase is $(1.2 \pm 0.1) \times 10^7$ $(M \cdot min)^{-1}$, and from the intercept the reverse rate constant is 0.18 ± 0.01 min^{-1} (which is in good agreement with values determined in dissociation experiments, Table I). Although all four data sets in Figure 2 require two exponentials to produce a good fit, the values of the rate constants for the slow phases are not determined with sufficient accuracy to apply an analysis like that of Figure 2C. However, the rate constants appear to be at most 10% of those of the fast phase.

The dissociation of dimer from $P388D_1$ cells was examined by the following procedure: cells were equilibrated with ^{125}I-labeled dimer, centrifuged, and resuspended without washing in either medium or medium containing monomeric IgG. This resulted in a 25–30-fold dilution of the unbound

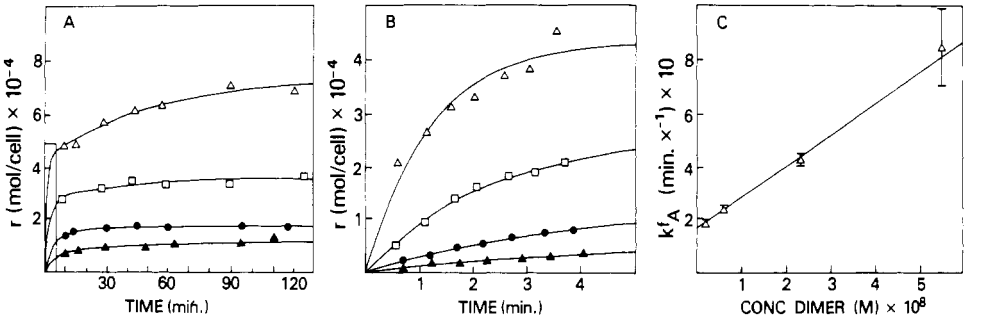

FIGURE 2: Association of BDPE dimer with P388D$_1$ cells at 0 °C. Association was measured with 6.1 × 10^6 cells/mL and (▲) 2.1 × 10^{-9}, (●) 6.1 × 10^{-9}, (□) 2.3 × 10^{-8}, and (△) 5.5 × 10^{-8} M BDPE dimer. Cell viability by trypan blue exclusion was 89%. The continuous curves drawn in (A) and (B) were calculated from a sum of two exponentials, with parameter values determined by least-squares fitting. (A) Whole time course, showing the data for the late time points. (B) Initial 5 min, showing the region of (A) enclosed in the box, with the data points included. (C) Plot of the apparent rate constants k_A^f (min^{-1}) for the fast-equilibrating component [determined by least-squares fits of eq 6 to the data in (A) and (B)] against the free dimer concentration. The error bars are the normal errors of the parameter values. The straight line shown was determined by least-squares fitting.

Table I: Analysis of BDPE Dimer Dissociation Data[a]

concn (M)	dimer subunits bound at 0 time	B_A^r	k_A^r (min^{-1})	B_B^r	k_B^r (min^{-1})
(A) Dissociation in the Absence of Monomer					
1.5 × 10^{-7} [b]	1.95 × 10^5	0.36	0.29	0.64	<1 × 10^{-2}
8.1 × 10^{-8} [b]	1.24 × 10^5	0.42	0.19	0.58	<1 × 10^{-2}
3.1 × 10^{-8} [b]	7.16 × 10^4	0.43	0.11	0.57	<1 × 10^{-2}
1.1 × 10^{-8} [b]	3.41 × 10^4	0.31	0.077	0.69	<1 × 10^{-2}
(B) Effect of Monomer on Dissociation of Dimer					
0	1.95 × 10^5	0.36	0.29	0.63	<1 × 10^{-2}
1.6 × 10^{-7} [c]	1.95 × 10^5	0.46	0.20	0.54	<1 × 10^{-2}
8.0 × 10^{-7} [c]	1.95 × 10^5	0.60	0.20	0.40	<1 × 10^{-2}
4.0 × 10^{-6} [c]	1.95 × 10^5	0.58	0.47	0.42	<1 × 10^{-2}
2.0 × 10^{-5} [c]	1.95 × 10^5	0.66	0.64	0.34	<1 × 10^{-2}

[a] The parameter values were obtained by least-squares fitting to the data of Figures 3 and 5A with eq 5. [b] Concentration of dimer in which the cells were preequilibrated. [c] Concentration of monomer in which the cells were resuspended.

dimer. The kinetics of release of bound dimer from cells equilibrated and resuspended in medium are shown in Figure 3. Good fits to the data were obtained with a sum of two exponentials (eq 5) and using three did not improve the fit. The relative amplitudes of the two processes (Table I) were similar at all dimer concentrations; the rate of the fast process decreased with decreasing initial receptor occupancy (the rate of the slow process is not accurately determined). In an equilibrium binding experiment (Figure 4), done with the same cells, the curvature in the Scatchard plot was almost entirely accounted for by multivalent binding of dimer to a single class of Fc receptors, unlike the preparations of cells used in the preceding paper in this issue (Dower et al., 1981). This suggested that heterogeneity in affinity was not the cause of the biphasic kinetics. Moreover, the ratio of the amplitude of the fast to the slow phase did not decrease systematically with decreasing initial levels of bound dimer, as would be expected if a high-affinity interaction gave rise to the slow release. In other experiments (data not shown), neither addition of unsheared salmon sperm DNA, to increase the viscosity of the medium, nor increasing the mixing rate of the cell suspension had any effect on the dissociation kinetics, indicating that diffusion effects were not influencing the behavior of the system. Further, since all the experiments were done at 0 °C, internalization did not contribute to the interaction of dimer with the cells (see below and Figure 6).

The addition of monomeric IgG to the medium accelerated the dissociation of dimer in a concentration-dependent manner (Figure 5A). The effect of monomer on the rate of dissociation of dimer paralleled its ability to inhibit dimer binding

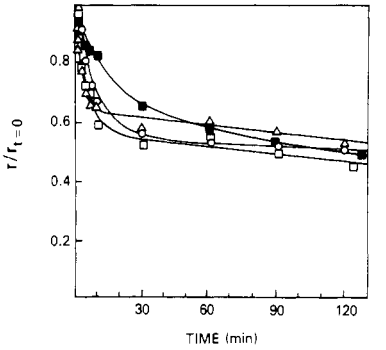

FIGURE 3: Dissociation of BDPE dimer from P388D$_1$ cells at 0 °C. Cells (8.5 × 10^6 cells/mL) were incubated 2 h at 0 °C with (▲) 1.5 × 10^{-7}, (□) 8.1 × 10^{-8}, (○) 3.1 × 10^{-8}, and (■) 1.1 × 10^{-8} M BDPE dimer, centrifuged, and resuspended in medium at zero time. Cell viability was 85% by trypan blue exclusion at the end of the experiment. To facilitate comparison of the four curves, we plotted the data in the form of $r/r_{t=0}$, where $r_{t=0}$ is the amount of dimer bound at zero time; $r_{t=0}$ values are given in Table IA. The continuous curves were calculated from the parameter values given in Table IA by using eq 5.

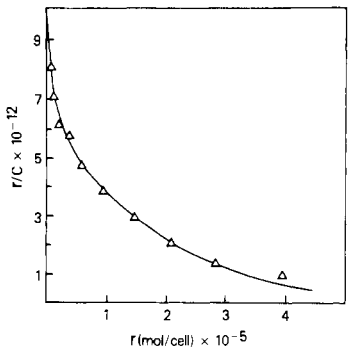

FIGURE 4: Equilibrium binding of BDPE dimer to P388D$_1$ cells at 0 °C. Data were collected with the same cell preparation used in the experiments of Figures 3 and 5. The data are plotted in Scatchard form, and the continuous curve was calculated from the multivalent binding model described by Dower et al. (1981), by using best-fit parameter values K_1 = 1.6 × 10^6 M^{-1}, K_2R_0 = 8.4, and r_0 = 4.1 × 10^5 (mol/cell) and a small number of receptors (7 × 10^3) binding dimer with much higher affinity.

at equilibrium (Figure 5B). Both the rapidly and slowly dissociating components were affected by monomeric IgG; this appeared in the analysis as a progressive increase in the relative amplitude of the rapid process with increasing monomer concentrations (Table I) and increases in the rate constants for the fast process. Similar effects were observed with cells preequilibrated in 1.1 × 10^{-8}, 3.1 × 10^{-8} or 8.1 × 10^{-8} M dimer (data not shown).

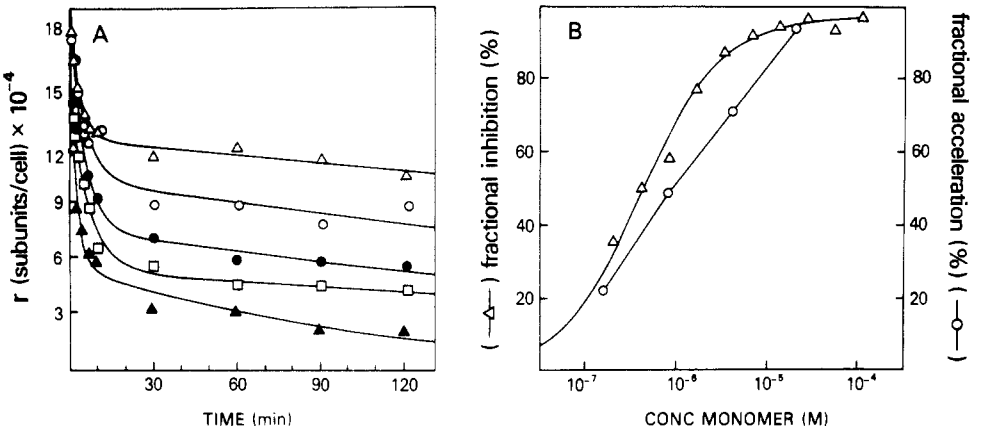

FIGURE 5: Effect of monomeric IgG on dissociation of BDPE dimer from P388D$_1$ cells at 0 °C. (A) Kinetics of dimer release. The experiment was done with the same cell preparation as in Figures 3 and 4. The cells were preequilibrated with 1.5×10^{-7} M dimer, pelleted, and resuspended in (△) 0, (○) 1.6×10^{-7}, (●) 8.0×10^{-7}, (□) 4.0×10^{-6}, or (▲) 2.0×10^{-5} M monomeric IgG. The continuous curves were calculated from a sum of two exponential terms by using the parameter values given in Table IB. (B) Comparison of the inhibition of equilibrium binding (△) with the acceleration of dissociation of dimer by monomeric IgG (○). Inhibition of binding was measured by using 1.4×10^{-8} M dimer. Fractional inhibition was calculated relative to dimer binding in the absence of monomer, and the continuous curve was calculated from a simple bimolecular model. The acceleration of dissociation was calculated from the data of Figure 5A and a similar data set collected with cells preequilibrated with 8.1×10^{-8} M dimer, as $(r_t - r_{tc})/r_t$, where r_t is the amount of dimer bound in the absence of monomer at time t and r_{tc} is the amount bound in the presence of a concentraton c of monomer. The points shown were averaged from data collected at 10, 60, and 120 min.

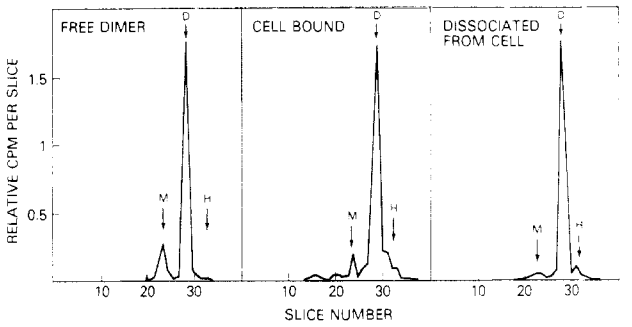

FIGURE 6: Polyacrylamide gel analysis of ^{125}I-labeled BDPE dimer. Electrophoresis was carried out on an 8-cm, 2–16% gradient slab gel in solution containing 0.2% sodium dodecyl sulfate. Individual tracks were sliced at 2-mm intervals and counted. Panels have been scaled to facilitate comparison. (A) Dimer prior to incubation with P388D$_1$ cells (1.8×10^5 cpm applied to gel). (B) Membrane-bound dimer. Dimer (2×10^{-7} M) was incubated with 6.8×10^7 cells in 1 mL of medium for 4 h at 0 °C. Cells were washed and lysed with NP-40, and the lysate was taken for analysis (3.41×10^4 cpm applied to gel). (C) Released dimer. Cells from (B) were incubated in medium at 0 °C for 1 h and centrifuged. An aliquot of medium was then taken for analysis (3.5×10^4 cpm applied to gel).

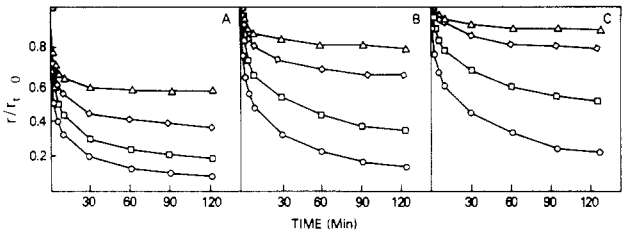

FIGURE 7: Dissociation of BDPE dimer, trimer, and Hmer from P388D$_1$ at 0 °C in the presence and absence of monomeric IgG. Cells (2.9×10^7 cells/mL, 89% viable by trypan blue exclusion) were incubated with (A) 2.0×10^{-7} M dimer, (B) 5.1×10^{-8} M trimer, (C) 1.8×10^{-8} M Hmer for 3 h, centrifuged, and resuspended in medium containing (△) 0, (◇) 4.2×10^{-7}, (□) 2.1×10^{-6}, and (○) 1.0×10^{-5} M monomeric IgG. Data are expressed as the fraction of bound subunits relative to the number of subunits bound prior to centrifugation ($r_{t=0}$). Values for $r_{t=0}$ were 1.2×10^5, 1.2×10^5, and 1.4×10^5 (mol/cell) for dimer, trimer, and Hmer, respectively.

At the highest monomer concentrations, >90% of the bound dimer dissociated from the cells, suggesting that the dimer had been neither internalized nor covalently linked to the cells. In order to determine the state of the bound dimer, we examined radiolabeled material bound to cells or eluted from cells by polyacrylamide gel electrophoresis under denaturing conditions. Migration patterns (Figure 6) showed that molecular weight distributions were similar for bound, released, and untreated dimer. Thus dimer was bound to the cells in an unaltered, releasable form.

Effect of Size on Dissociation of BDPE Cross-Linked Oligomers from P388D$_1$ Cells at 0 °C. Figure 7 shows the dissociation of BDPE cross-linked radiolabeled dimer, trimer and "Hmer" from P388D$_1$ cells at 0 °C in the presence of sodium azide. The Hmer preparation is a mixture of predominantly trimer (22.1%) and tetramer (44.0%) with ~15% each of monomer and dimer, determined by NaDodSO$_4$–polyacrylamide gel electrophoresis. The dimer and trimer preparations have been described in the previous paper (Dower et al., 1981). The protocol for the experiment shown in Figure 7 was the same as that described for dimer. Briefly, cells were equilibrated with radiolabeled oligomer, centrifuged, and resuspended without washing, either in medium alone or in medium containing unlabeled monomeric IgG. The data in Figure 7 show that for all three oligomers, the presence of high concentrations of monomeric IgG leads to a marked enhancement in dissociation. This enhancement decreases with oligomer size; the concentrations of monomer required to produce half the maximal enhancement were 9.1×10^{-7}, 1.2×10^{-6}, and 1.8×10^{-6} M for dimer, trimer, and Hmer, respectively. The rates of dissociation of the oligomers, after dilution alone, also decreased with size. Comparison of the trimer and tetramer data, in particular, suggests that the tetramer component in the Hmer is barely released at all from the cells in 2 h.

Comparison of Dissociation of DIBADL and BDPE Cross-Linked Dimers from P388D$_1$ Cells at 0 °C. In the preceding paper in this issue (Dower et al., 1981), we suggested that DIBADL oligomers aggregate into larger noncovalent complexes on the cell surface. DIBADL dimer might, therefore, be expected to dissociate from the cell surface more slowly than BDPE dimer, which does not aggregate, since the rate of dissociation of an oligomer decreases inversely with the number of IgG subunits in it (Figure 7). The data in Figure 8 show that this is the case. Here, cells were preequilibrated

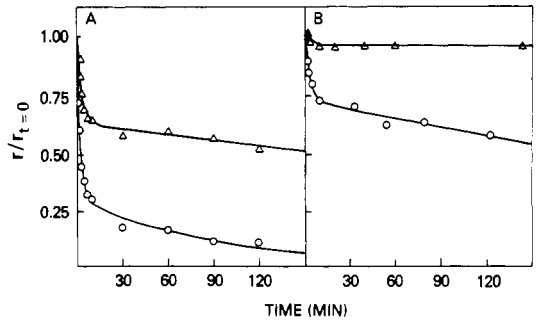

FIGURE 8: Comparison of dissociation of (A) BDPE dimer and (B) DIBADL dimer from P388D$_1$ cells at 0 °C. (A) Cells (8.5×10^6 cells/mL, 85% viable by trypan blue exclusion) were preequilibrated with 1.5×10^{-7} M BDPE dimer at 0 °C, spun, and resuspended in (△) medium and (○) medium with 2×10^{-5} M monomeric IgG. (B) Cells (1.4×10^7 cells/mL, 93% viable by trypan blue exclusion) were incubated with 3.8×10^{-8} M DIBADL dimer in the presence of 10^{-4} M Dnp-ε-aminocaproate at 0 °C for 2 h, centrifuged, and resuspended in (△) medium containing 10^{-4} Dnp-ε-aminocaproate or the same medium with 2.8×10^{-5} M monomeric IgG (○).

with either BDPE or DIBADL dimer, centrifuged, and resuspended in medium alone or in medium containing a high concentration of monomeric IgG. Approximately 50% of the bound BDPE dimer was released within 2 h after the cells were resuspended in medium, but only 5% of the DIBADL dimer was released. Moreover, the DIBADL dimer dissociated less rapidly than BDPE dimer in the presence of a high concentration of monomeric IgG. Comparison of the data for DIBADL dimer (Figure 8B) with those for BDPE Hmer (Figure 7C) suggests that nearly all the cell-associated DIBADL dimer was in the form of tetramers (i.e., two noncavalently linked dimers) or larger aggregates.

Discussion

The binding of immune complexes to Fc receptors on endocytic cells such as P388D$_1$ is the first step in an irreversible sequence of processes leading to internalization and degradation. The whole endocytic process never reaches equilibrium under physiological conditions; hence, the rates of the individual steps are more biologically relevant than the equilibrium states. In this paper we have studied the kinetics of the initial step of endocytosis by metabolically inhibiting subsequent steps. Under these conditions the association of oligomers with receptors reaches a plateau (Figure 2), and bound oligomer can be largely displaced from the cell surface in an intact form (Figures 5–8). Fc receptors on metabolically inhibited P388D$_1$ cells thus come into equilibrium with oligomers from the fluid phase, and the multivalent binding model which describes the equilibrium state (Dower et al., 1981) also predicts the behavior of the system as it approaches equilibrium.

The observation that the rate of dissociation of cell-bound oligomers is accelerated by adding monomeric IgG to the cell suspension (thus decreasing R_f) allows us to estimate some of the rate constants of eq 1 and to determine the rate-limiting process for association. Figure 1 and eq 4 show that in order for the acceleration of dimer release to occur, the rate at which monovalently bound dimer (D_1) becomes divalently bound must be rapid compared with the rate at which D_1 dissociates from the cell surface, i.e.

$$k_{-1} < k_2 R_f \tag{8}$$

In our association experiments (Figure 2), the maximum concentration of free dimer was $\sim 5 \times 10^{-8}$ M. The equilibrium constant, K_1, for the first step in dimer binding is $\sim 10^6$ M^{-1} (Dower et al., 1981), and therefore

$$2K_1 D < 0.1 \tag{9}$$

Since $K_1 = k_1/k_{-1}$ and from eq 8, it follows that

$$2k_1 D < 0.1k_{-1} < k_2 R_f \tag{10}$$

Because $2k_1 D$ is the pseudo-first-order rate constant for the first step of dimer binding ($D \rightarrow D_1$) and $k_2 R_f$ is the rate of the second step ($D_1 \rightarrow D_2$), these inequalities demonstrate that in the association experiment (Figure 2), the first step is rate limiting. The rate constant determined for the rapid component (Figure 2C) is therefore equivalent to $2k_1$. The calculated values for k_1 and k_{-1} (determined from K_1) are 6×10^6 $(M \cdot min)^{-1}$ and 4 min^{-1}, respectively, and, in addition, $k_2 R_f$ must be at least 40 min^{-1} to account for the acceleration of dimer release by monomeric IgG.

The reason that the first step in dimer binding is rate limiting most probably derives from the relative differences in ligand concentrations available to free receptors, when binding occurs from bulk solution ($D \rightarrow D_1$) or when binding occurs on the cell surface ($D_1 \rightarrow D_2$). Cell surface concentrations of ligand may be several orders of magnitude greater than those in solution phase (Cohen & Eisen, 1977; Dower et al., 1981). Cross-linking rates should, therefore, be greater than the rates of forming the first bond with ligand from solution for most cases of multivalent binding.

The binding of oligomers to the cells could be diffusion limited; this is, however, unlikely. The rate of diffusion of dimer from solution to the surface of a spherical cell 5 μm in diameter can be calculated from the relation $k_f = 4\pi Da$ (Noyes, 1961), where a is the cell radius and D is the ligand diffusion coefficient. Assuming a value of 5×10^{-6} cm^2 min^{-1} for D, the diffusion-limited association rate is 10^{12} $(M \cdot min)^{-1}$. The measured value [6×10^6 $(M \cdot min)^{-1}$] is several orders of magnitude less than this. Similarly, by use of the relationship $k_r = 3D/a^2$ (Noyes, 1961), the calculated rate of diffusion of dimer away from the cell surface (assuming no rebinding; Berg & Purcell, 1977) would be 6×10^3 min^{-1}. Since the maximum estimated value (4 min^{-1}) is much less, k_{-1} is also probably not limited by diffusion. Further, we found that neither altering the viscosity of the medium nor vigorous mixing of the cell suspension affected the kinetics of interaction of dimer with Fc receptors on P388D$_1$ cells. This also indicates that diffusion in solution is not rate limiting in dimer binding or dissociation.

Since the cross-linking step, $D_1 \rightarrow D_2$, is not rate limiting, the rate of receptor diffusion in the plane of the cell membrane will not affect the dimer association rate. However, this step does influence the dissociation rates when $k_2 R_f$ is large. The diffusion-limited rate of cross-linking, $k_2 R_f$, calculated for a cell 5 μm in diameter containing 10^5 free Fc receptors per cell with a two-dimensional diffusion coefficient of 10^{-10} cm^2/s^{-1} (Berg & Purcell, 1977; Dragsten et al., 1979), is 3000 min^{-1}. From the kinetics experiments, we can only determine that $k_2 R_f$ must be >40 min^{-1}; hence its value must lie somewhere in the range 40–3000 min^{-1}.

Simulations using the complete set of differential equations describing the binding mechanism (eq 3) confirmed that under all conditions where monomeric IgG accelerates the rate of release of dimer, $k_2 R_f$ must be greater than k_{-1}. No simulated conditions could be found where both $k_2 R_f$ was greater than k_{-1} and the dissociation was biphasic. The observations that both association and dissociation occur by at least two processes and that monomeric IgG accelerates dissociation are, therefore, inconsistent with the simplest mechanism. The multiphase kinetics do not derive from heterogeneity in binding constants, since the cell preparation used in Figures 3 and 5 exhibited no such heterogeneity (Figure 4), and the relative rates of fast and slow processes were largely independent of

the concentration of dimer with which the cells were initially equilibrated. A plausible explanation for the biphasic kinetics of association and dissociation is that some of the Fc receptors are less accessible to the bulk medium than others. This could occur, for example, if receptors were temporarily sequestered in membrane folds. Such an effect would reduce both on and off rates of a fraction of the receptors, without necessarily producing heterogeneity in the equilibrium binding. In our experiments ~65% of the dimer molecules associated with cells at the fast rate, while only 35% dissociated rapidly. In an equilibrating system, however, the dissociation rate is likely to be higher than in the experiments illustrated in Figure 3, since free dimer in solution would accelerate the dissociation process. Multiexponential kinetics have been observed in several other cell surface receptor–ligand systems, and in these systems also, the origin of the complexity in the kinetics has not been fully accounted for (DeMeyts et al., 1973; Frazier et al., 1974; DeMeyts, 1976; Segal & Hurwitz, 1977; Boyd & Cohen, 1980; Landreth & Shooter, 1980; Mason & Williams, 1980).

The decrease in the rate of dissociation of the BDPE oligomers with increasing oligomer size (Figure 7) is also consistent with the cross-linking mechanism, since larger oligomers will bind to more Fc receptors (Dower et al., 1981) and, therefore, more ligand–receptor bonds will have to be broken in order for the oligomer to dissociate from the cell. Because self-aggregation increases the effective oligomer size on the cell surface, DIBADL dimers dissociate more slowly than those cross-linked with BDPE (Figure 8). Immune complexes, which can be large and self-aggregating might therefore be expected to remain cell associated for long periods of time if they should become cell bound in vivo.

The data presented in this paper were collected at 0 °C in the presence of sodium azide in order to prevent internalization and degradation of the IgG oligomers by the $P388D_1$ cells. Most probably, the rates of the processes measured here are slower than at 37 °C, the physiological temperature. However, several features of the system are likely to be the same at the two temperatures; in particular, the rate of the initial reaction between oligomers and cell surface Fc receptors will probably be rate limiting at 37 °C, and the rate of oligomer dissociation will decrease with increasing oligomer size and with self-aggregation. Physiological concentrations of IgG (~10 mg/mL; Spiegelberg, 1974) will greatly retard the rates of association of oligomers of all sizes with cells, by competing with the oligomers for free Fc receptors. Such competition will occur at both the initial monovalent binding step and at subsequent cross-linking steps. However, the second and subsequent subunits of bound oligomers should be able to compete effectively with solution phase IgG for free receptors, because the local concentrations of these subunits relative to the receptors will be higher. As a result, oligomers of all sizes will undergo several cycles of multivalent binding before passing through the monovalent intermediate and dissociating from the cell. Oligomers should therefore reside on the cell surface for a longer average time than the monomeric protein, and this effect should increase with oligomer size and with self-aggregation. In physiological processes such as internalization of immune complexes or stimulation of exocytosis, the resident mean lifetime on the cell of multivalent immune complexes could be more important than the level of binding at equilibrium (Bergman & Hechter, 1978; DeLisi, 1981).

Acknowledgments

We thank Dr. Gary Knott for extensive help with MLAB and Drs. Pierre Henkart, Richard Klausner, and David Sachs for thoughtful reading of the manuscript.

References

Berg, H. F., & Purcell, F. N. (1977) *Biophys. J. 20*, 193–219.
Bergman, R., & Hechter, O. J. (1978) *J. Biol. Chem. 253*, 3238–3249.
Boyd, N. D., & Cohen, J. B. (1980) *Biochemistry 19*, 5353–5358.
Cohen, R. J., & Eisen, H. N. (1977) *Cell. Immunol. 32*, 1–9.
DeLisi, C. (1978) in *Physical Chemical Aspects of Cell Surface Events in Cellular Regulation* (DeLisi, C., & Blumenthal, R., Eds.) Vol. 4, pp 261–285, Elsevier/North-Holland, New York.
DeLisi, C. (1981) *Nature (London) 289*, 322–323.
DeMeyts, P. (1976) *J. Supramol. Struct. 4*, 241–258.
DeMeyts, P., Roth, J., Neville, D. M., Sr., Gam, J. R., III, & Lesniack, M. A. (1973) *Biochem. Biophys. Res. Commun. 55*, 154–161.
Dower, S. K., DeLisi, C., Titus, J. A., & Segal, D. M. (1981) *Biochemistry* (preceding paper in this issue).
Dragsten, P., Henkart, P., Blumenthal, R., Weinstein, J., & Schlessinger, J. (1979) *Proc. Natl. Acad. Sci. U.S.A. 76*, 5163–5167.
Frazier, W. A., Boyd, L. F., & Bradshaw, R. A. (1974) *J. Biol. Chem. 249*, 5513–5519.
Jencks, W. P. (1969) *Catalysis in Chemistry and Enzymology*, pp 568–590, McGraw-Hill, New York.
Jones, J. F., Plotz, P. H., & Segal, D. M. (1979) *Mol. Immunol. 16*, 889–897.
Knott, G. D. (1979) *Comput. Programs Biomed. 10*, 271–280.
Landreth, G. E., & Shooter, E. N. (1980) *Proc. Natl. Acad. Sci. U.S.A. 77*, 4751–4755.
Mason, D. W., & Williams, A. F. (1980) *Biochem. J. 187*, 1–20.
Noyes, R. M. (1961) *Prog. React. Kinet. 1*, 129–160.
Segal, D. M., & Hurwitz, E. (1977) *J. Immunol. 118*, 1338–1347.
Silverstein, S. C., Steinman, R. M., & Cohn, Z. A. (1977) *Annu. Rev. Biochem. 46*, 669–722.
Spiegelberg, H. L. (1974) *Adv. Immunol. 19*, 259–294.